Correlation of angiogenesis with ^{18}F-FMT and ^{18}F-FDG uptake in non-small cell lung cancer

Kyoichi Kaira,[1,8] Noboru Oriuchi,[2] Kimihiro Shimizu,[3] Tomohiro Ishikita,[4] Tetsuya Higuchi,[2] Hisao Imai,[1] Noriko Yanagitani,[1] Noriaki Sunaga,[1] Takeshi Hisada,[1] Tamotsu Ishizuka,[1] Yoshikatsu Kanai,[5] Hitoshi Endou,[6] Takashi Nakajima,[7] Keigo Endo,[2] and Masatomo Mori[1]

[1]Department of Medicine and Molecular Science, [2]Department of Diagnostic Radiology and Nuclear Medicine, [3]Department of Thoracic and Visceral Organ Surgery, [4]Department of Stomatology and Maxillofacial Surgery and [7]Department of Tumor Pathology, Gunma University Graduate School of Medicine, Showa-machi, Maebashi, Gunma 371-8511, Japan; and [5]Division of Bio-system Pharmacology, Department of Pharmacology, Osaka University Graduate School of Medicine, 2-2 Yamadaoka, Suita, Osaka 565-0871, Japan; and [6]Department of Pharmacology and Toxicology, Kyorin University School of Medicine, Shinkawa, Mitaka, Tokyo 181-8611, Japan

(Received October 29, 2008/Revised December 1, 2008/Accepted December 7, 2008/Online publication January 12, 2009)

L-[3-^{18}F]-α-methyltyrosine (^{18}F-FMT) is an amino-acid tracer for positron-emission tomography (PET). We have conducted a clinicopathologic study to elucidate the correlation of angiogenesis with ^{18}F-FMT and 2-[^{18}F]-fluoro-2-deoxy-D-glucose (^{18}F-FDG) uptake in patients with non-small cell lung cancer (NSCLC). Thirty-seven NSCLC patients were enrolled in this study, and two PET studies with ^{18}F-FMT and ^{18}F-FDG were performed. Uptake of PET tracers was evaluated with standardized uptake value. Vascular endothelial growth factor (VEGF), CD31, CD34, L-type amino acid transporter 1 (LAT1) and Ki-67 labeling index of the resected tumors were analyzed by immunohistochemical staining, and correlated with the clinicopathologic variables and the uptake of PET tracers. The median VEGF rate was 45% (range, 10–78%). High expression was seen in 30 patients (81%, 30/37). VEGF expression was statistically associated with progressively growing microvessel count. VEGF showed a correlation with LAT1 expression ($P = 0.04$) and Ki-67 labeling index ($P = 0.01$). However, it showed no correlation with age, gender, disease stage, tumor size, and histology. Microvessel density (MVD) showed no correlation with any parameters. ^{18}F-FMT and ^{18}F-FDG uptake correlated significantly with VEGF ($P < 0.0001$, $P = 0.026$, respectively), whereas the correlation of ^{18}F-FMT and VEGF was more meaningful. The present study demonstrated that the metabolic activity of primary tumors as evaluated by PET study with ^{18}F-FMT and ^{18}F-FDG is related to tumor angiogenesis and the proliferative activity in NSCLC. (*Cancer Sci* 2009; 100: 753–758)

Tumor angiogenesis is an essential requirement for the development, progression, and metastasis of malignant tumors. Several reports have stated that the presence of angiogenesis is a significant prognostic factor in terms of overall and disease-free survival in lung cancer.[1,2] Tumor vasculature is analyzed by immunohistochemical staining with vascular endothelial growth factor (VEGF)[3] and the microvessel density (MVD) as determined by CD31 and CD34 expression in archival tumor material.[1,2] VEGF is a glycoprotein with potent angiogenic, mitogenic, and has vascular permeability-enhancing activity in endothelial cells. CD31 and CD34 are endothelial antigens that have been used to represent the density of intratumor vessels as a direct marker of angiogenesis.

The usefulness of positron emission tomography with 2-[^{18}F]-fluoro-2-deoxy-D-glucose (^{18}F-FDG PET) has been investigated in the diagnosis of non-small cell lung cancer (NSCLC).[4,5] Determination of malignant lesions with ^{18}F-FDG PET is based on glucose metabolism.[6] The overexpression of glucose transporter 1 (Glut1) has been shown to be closely related to ^{18}F-FDG uptake, and ^{18}F-FDG uptake is a significant prognostic factor in patients with NSCLC.[7,8] There is a report regarding the correlation between MVD and ^{18}F-FDG uptake in NSCLC.[9] However, it is not yet conclusive whether there is any correlation between ^{18}F-FDG uptake and the expression of VEGF or MVD.

We have been conducting PET studies using L-[3-^{18}F]-α-methyltyrosine (^{18}F-FMT), which is supposed to be accumulated in the tumor cells solely via an amino-acid transport system.[10,11] The studies have demonstrated that ^{18}F-FMT PET is useful to differentiate between benign lesions and malignant tumors, including lung cancer.[12,13] Recently, we have reported that uptake of ^{18}F-FMT in tumors is closely correlated with L-type amino acid transporter 1 (LAT1) expression in NSCLC.[14] LAT1 is widely expressed in primary human cancers and several cancer cell lines, where it has been shown to play essential roles in the growth of tumor and the survival of patients.[15] Although LAT1 expression seems to correlate with the metastatic mechanism, it is unknown whether there is any correlation between LAT1 expression and tumor angiogenesis.

Recently, the targeted therapy against endothelial growth factor has been shown to have a potential to improve outcome in patients with NSCLC.[16] Bevacizumab, a recombinant humanized monoclonal anti-VEGF antibody, is used for the treatment of NSCLC.[16] However, it is uncertain whether PET is useful for monitoring the response to the targeted therapy against VEGF. To explore the clinical significance of PET using ^{18}F-FMT and ^{18}F-FDG for monitoring anti-VEGF-directed, targeted therapies, we have conducted a clinicopathologic study to elucidate the correlation of angiogenesis with ^{18}F-FMT and ^{18}F-FDG uptake in patients with NSCLC.

Methods

Patients. Thirty-seven patients (24 men and 13 women: age 42–80 years; mean age, 64 years) with NSCLC were enrolled in this study. The study was conducted at the Gunma University Hospital, Japan, a teaching and tertiary care hospital and a major referral site for patients with lung cancer. All consecutive patients referred for surgery from November 2005 to January 2007 were included in the study. Histological analysis revealed adenocarcinoma (AC) in 18 patients, squamous cell carcinoma (SQC) in 15, large cell carcinoma (LCC) in two, and others in two. All patients underwent a thoracotomy within 4 weeks after the ^{18}F-FMT PET and ^{18}F-FDG PET studies. No patient had received neoadjuvant chemotherapy or radiotherapy before surgery. Final diagnoses were established histologically (via the thoracotomy) in all patients, and the pathologic staging was conducted in accordance with internationally accepted staging guidelines.

Our clinical trial registration number is ClinicalTrials.gov ID: NCT00671242

[8]To whom correspondence should be addressed. E-mail: kkaira1970@yahoo.co.jp

doi: 10.1111/j.1349-7006.2008.01077.x

None of the patients had insulin-dependent diabetes, and the serum glucose levels in all patients just before ^{18}F-FMT and ^{18}F-FDG injection were less than 120 mg/dL. All patients agreed to participate in these studies and provided written informed consent. The study protocol was approved by the institutional review board.

PET studies. ^{18}F-FMT was synthesized in our cyclotron facility according to the method developed by Tomiyoshi *et al*.[17] Radiochemical yield of ^{18}F-FMT was approximately 20% and radiochemical purity was approximately 99%. ^{18}F-FDG was also produced in our facility as described previously.[18] The patients were fasted for at least 6 h before the PET studies. PET study was performed using a whole-body PET scanner with BGO ($Bi_4Ge_3O_{12}$) crystals (SET 2400 W; Shimadzu, Kyoto, Japan) with 59.5 cm transverse fields of view, which produced 63 image planes with a 3.123-mm interval between images. Transverse resolution at the center of the field of view was 4.2 mm full width half maximum.

Two-dimensional data acquisition was initiated 50 min after the injection of 4–5 MBq/kg or 5–6 MBq/kg of ^{18}F-FMT or ^{18}F-FDG, respectively, as described previously.[19] The image protocol was set to use a simultaneous emission-transmission method with a rotating external source (370 MBq of ^{68}Ge-^{68}Ga at the time of installation) and to acquire 4–10-bed positions (8-minute acquisition per bed position) according to the range of imaging. In cases of bone and skin lesions in the extremities, a maximum of 10-bed positions was acquired to cover the whole body. Attenuation-corrected transverse images were reconstructed with the ordered-subsets expectation maximization algorithm into 128×128 matrices with pixel dimensions of 4.0 mm in-plane and 3.125 mm axially. Coronal images with a 9.8-mm section thickness were also reconstructed from attenuation-corrected transverse images for visual interpretation.

Data analysis. All ^{18}F-FDG and ^{18}F-FMT PET images were interpreted by two experienced nuclear physicians. The interpreting physicians were unaware of the patients' clinical histories and data. Moderate uptake and intense uptake were defined as positive results of visual interpretation, and faint uptake and no uptake which were less than the uptake in the normal mediastinum were defined as negative results. Discrepant results were resolved by the consensus review. For the semiquantitative analysis, functional images of the standardized uptake value (SUV) were produced using attenuation-corrected transaxial images, injected doses of ^{18}F-FMT and ^{18}F-FDG, patient body weight, and the cross-calibration factor between PET and dose calibrator.[19] SUV was defined as follows:

SUV = Radioactive concentration in the region of interest (ROI) [MBq/g]/Injected dose (MBq)/Patient's body weight.

Regions of interest of approximately 1 cm in diameter were manually drawn on the SUV images over the area corresponding to the maximal tracer uptake in the lesions, when multiple lesions were present, or the lesion was >1 cm in diameter. SUV of background was defined by drawing ROI at the site other than lymphadenopathy in the mediastinum. When the lesion showed no significant tracer uptake, ROI was placed retrospectively on the PET image with reference to the CT image. ROI analysis was conducted by a nuclear physician with the aid of corresponding CT scans. The maximal SUV in the ROI was used as a representative value for the assessment of ^{18}F-FMT and ^{18}F-FDG uptake in the lesion.

Immunohistochemical staining. VEGF, CD31, and CD34. Immunohistochemical staining for VEGF, CD31, and CD34 was performed by the avidin-biotin method. In brief, sections were deparaffinized with xylene and rehydrated with ethanol. For VEGF, the sections were trypsinized, and incubated with blocking serum. For CD31, antigen retrieval was done by placing the specimen in 0.01 mol/L of citrate buffer at pH 6.0 and exposing it to microwave heating of 20 min at 450 W. For CD34, the sections were treated by protease.

The antibodies used were: a monoclonal antibody against VEGF (Immuno-Biological Laboratories Co., Ltd, Takasaki, Gunma, Japan, 1:100 dilution); a mouse monoclonal antibody against CD31 (Dako, 1:50 dilution); and a mouse monoclonal antibody against CD34 (Nichirei, Tokyo, Japan, 1:200 dilution).

Expression of VEGF and vessel count was evaluated by two investigators without knowledge of patient outcomes. The expression of VEGF was assessed according to the percentage of immunoreactive cells in a total of 1000 neoplastic cells (quantitative analysis). The cutoff point to distinguish low from high VEGF expression was 25% of positive carcinoma cells as described previously.[20] There was >95% agreement between the two observers for the VEGF evaluation. A final score was determined by consensus after re-evaluation. We categorized the patients according to the percentage of tumor staining cells as follows: score 1, 0–25%; score 2, 25–50%; and score 3, >50%.

Microvessel density was assessed using the criteria of Weidner *et al*.[21] The areas of highest neovascularization were identified as regions of invasive carcinoma with the highest numbers of discrete microvessels stained for CD31 and CD34. Any brown-stained endothelial cell or endothelial cell cluster that was clearly separate from adjacent microvessels, tumor cells, and other connective tissue elements was considered a single, countable microvessel. Microvessels in sclerotic areas within the tumor, where microvessels were sparse, and immediately adjacent areas of unaffected lung tissue, were not considered in vessel counts. The number of CD31- and CD34-positive vessels was counted in four selected hot spots in a ×400 field (0.26 mm^2 field area). The mean value of the two independent readings of the same specimen was calculated, and MVD was defined as the mean count of microvessels per 0.26 mm^2 field area.[22]

Ki-67. The detailed protocol for immunostaining was published elsewhere.[23] Briefly, formalin-fixed and paraffin-embedded sections of resected specimens were dewaxed, rehydrated, trypsinized, and boiled in 0.01 mol/L citrate buffer for 20 min. For immunostaining, the murine monoclonal antibody molecular immunology borstel-1 (MIB-1) (Dako, Glostrup, Denmark), specific for human nuclear antigen Ki-67, was used in a 1:40 dilution. The sections were lightly counterstained with hematoxylin. Sections of a normal tonsil were used as positive control for proliferating cells.

A highly cellular area of the stained sections was evaluated. All epithelial cells with nuclear staining of any intensity were defined as positive. Approximately 1000 nuclei were counted on each slide. Proliferative activity was assessed as the percentage of MIB-1-stained nuclei (Ki-67 labeling index) in the sample. Ki-67 expression was defined as low if less than 25% of tumor cells showed nuclear staining in a tumor section. This definition was used according to the commonly used cutoff values ranging from 20–40% in NSCLC and other human cancers in the current literature[24] and also based on the examination of our staining data. Sections were evaluated by two investigators separately and in case of discrepancies both would evaluate the slide simultaneously and would agree in their final assessment. Neither investigator had knowledge of patient outcome.

LAT1. LAT1 expression was determined by immunohistochemical staining with an affinity-purified rabbit polyclonal anti-human LAT1 antibody.[25] An oligopeptide corresponding to amino acid residues 497–507 of human LAT1 (CQKLMQVVPQET) was synthesized. The N-terminal cysteine residue was introduced for conjugation with keyhole limpet hemocyanine. Antipeptide antibody was produced as described elsewhere.[26] For immunohistochemical analysis, antiserum was affinity-purified as described previously.[26]

Immunohistochemical staining was performed on paraffin sections using a polymer peroxidase method (Envision +/horseradish peroxidase; Dako Cytomation, Glostrup, Denmark). Briefly, deparaffinized, rehydrated sections were treated with 0.3% hydrogen peroxide in methanol for 30 min to block endogenous

doi: 10.1111/j.1349-7006.2008.01077.x

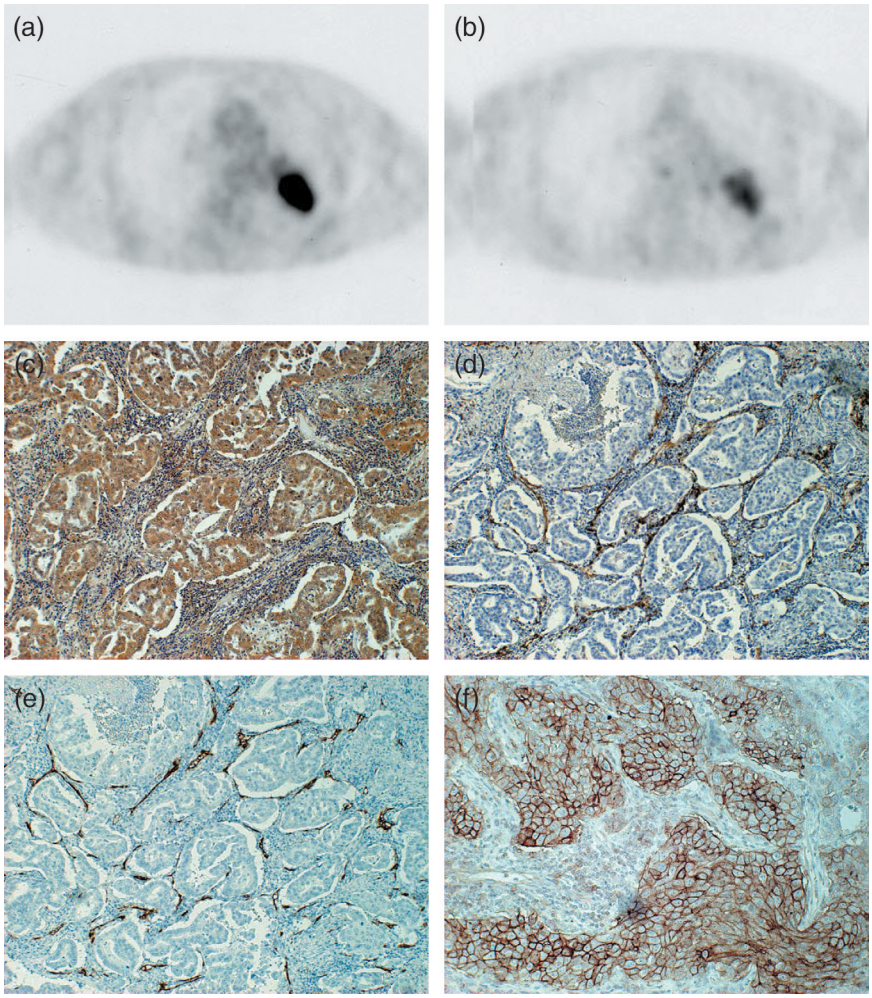

Fig. 1. Transaxial sections of 2-[^{18}F]-fluoro-2-deoxy-D-glucose positron-emssion tomography (^{18}F-FDG PET) (a) and L-[3-^{18}F]-α-methyltyrosine PET (^{18}F-FMT PET) (b) of a 74-year-old man with adenocarcinoma of the left lung (p-T2N0M0). Tumoral ^{18}F-FDG and ^{18}F-FMT uptake is intense with standardized uptake value (SUV) = 11.5 and SUV = 2.65, respectively. Immunostaining for vascular endothelial growth factor (VEGF) (c) reveals that more than 80% of tumor cells show positive reaction for anti-VEGF antibody. Immunostaining for CD31 (d) and CD34 (e) reveal that many small vessels with positive CD31 or CD34 are seen in the stroma of tumor tissue. The scoring of L-type amino acid transporter 1 immunostaining was grade 4 and its immunostaining pattern was membranous (f).

peroxidase activity. To expose antigens, sections were autoclaved in 10 mmol/L sodium citrate buffer (pH 6.0) for 5 min, and cooled for 30 min. After rinsing in 0.05 M tris-buffered saline containing 0.1% tween-20, the sections were incubated with affinity purified anti-LAT1 antibody (1.2 mg/mL; 1:3200) overnight at 4°C. Thereafter, they were incubated with Envision (++) rabbit peroxidase (Dako, Carpinteria, CA, US) for 30 min. The peroxidase reaction was performed using 0.02% 3,3′-diaminobenzidine tetrahydrochloride and 0.01% hydrogen peroxide in 0.05 mol/L tris-HCl buffer, pH 7.4. Finally, nuclear counterstaining was performed with Mayer's hematoxylin. For the negative control, the incubation step with the primary antibody was omitted. The specificity of immunoreactions using the anti-LAT1 antibody was established in previous studies.[27,28]

LAT1 expression was considered positive only if distinct membrane staining was present. Staining intensity was scored as follows: 1, <10% of tumor area stained; 2, 11–25% stained; 3, 26–50% stained; and 4, ≥51% stained. The tumors in which stained tumor cells made up more than 25% of the tumor were graded as positive. According to this scoring protocol, two investigators from the authors, without prior knowledge of the clinical data, independently graded the staining intensity in all cases. To test the intra-observer variability, each section was reassessed by the same investigators after the first assessment had been completed. The time interval between the first and second assessments was at least 4 weeks. The inter-observer variability was also determined by comparing the values of the first measurements of two investigators.

Statistical analysis. Data are presented as mean, range, and SD. Probability values of <0.05 indicated a statistically significant difference. Fisher's exact test was used to examine the association of two categorical variables. Correlation between maximal SUV and the levels of immunohistochemical staining of VEGF, CD31, CD34, LAT1, or Ki-67 was analyzed using the non-parametric Spearman's rank test. Statistical analysis was performed using StatView J-4.5 for Macintosh.

Results

^{18}F-FDG and ^{18}F-FMT uptake were evaluated for the primary tumor. VEGF, CD31, CD34, LAT1, and Ki-67 immunohistochemical staining were evaluated for the surgically resected 37 primary lesions.

Correlation between VEGF expression and tumor microvessel count. To investigate the clinical significance of VEGF expression in NSCLC, immunohistochemical staining was performed on the resected specimens of 37 patients using an antibody specific to VEGF. The staining pattern of VEGF was uniformly localized in the cytoplasm as shown in Fig. 1(c). The median rate of VEGF positivity was 45% (range, 10–78%). High expression was seen in 30 patients (81%, 30/37).

We next assessed the association of VEGF expression and MVD in primary tumors. The median rate of MVD as assessed by CD31 was 21 (range, 0–56), and the value of 20 was chosen as the cutoff point. High expression was seen in 21 patients (57%, 21/37). The median rate of MVD as assessed by CD34

Table 1. Relationship of clinicopathological parameters to angiogenesis

Parameter	VEGF			CD31-MVD			CD34-MVD		
	Low	High	*P*-value	Low	High	*P*-value	Low	High	*P*-value
All patients	7	30		16	21		12	25	
Age									
≤65 years	4	7	0.16	2	9	0.07	3	8	0.66
>65 years	3	23		14	12		9	17	
Gender									
Male	3	22	0.18	13	11	0.09	10	15	0.26
Female	4	8		3	10		2	10	
Tumor size (mm)									
≤30	3	13	0.98	7	10	0.82	4	12	0.49
>30	4	17		9	11		8	13	
Histology									
Adenocarcinoma	5	13	0.23	6	12	0.32	4	14	0.29
Non-adenocarcinoma	2	17		10	9		8	11	
Disease stage (p-stage)									
I	4	16	0.86	9	11	0.82	4	15	0.17
II + III	3	14		7	10		8	10	
LAT1									
Positive	1	18	0.04	7	12	0.51	6	13	0.80
Negative	6	12		9	9		5	13	
Ki-67 labeling index									
High	3	27	0.01	13	18	0.72	10	21	0.96
Low	4	3		3	3		2	4	

Abbreviation: Non-adenocarcinoma, non-small cell lung cancer except for adenocarcinoma; LAT1, L-type amino acid transporter 1; VEGF, vascular endothelial growth factor; MVD, microvessel density.

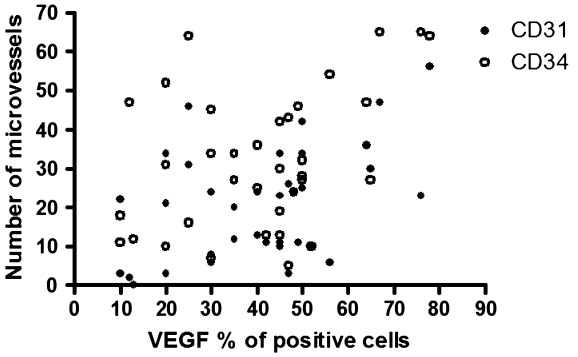

Fig. 2. Relationship between microvessel count as determined with CD31 or CD34 immunostaining and vascular endothelial growth factor (VEGF) expression in non-small cell lung cancer (NSCLC) (CD31-microvessel density [MVD] [$\gamma = 0.4258$, $P = 0.008$] and CD34-MVD [$\gamma = 0.3305$, $P = 0.045$]).

was 31 (range, 10–65) and the value of 30 was chosen as the cutoff point. High expression was seen in 25 patients (68%, 25/37). The analysis of the relationship between VEGF expression and the number of microvessels in the areas of the highest vascularization showed a significant association between mean microvessel count and VEGF expression in the tumor. As shown in Fig. 2, an increase in the VEGF expression was statistically associated with the number of microvessel count (CD31-MVD [$\gamma = 0.4258$, $P = 0.008$] and CD34-MVD [$\gamma = 0.3305$, $P = 0.045$], respectively).

Correlation between angiogenesis and clinicopathologic parameters. Table 1 shows the results of a comparison between clinicopathologic parameters including LAT1 expression and Ki-67 labeling index and VEGF expression, MVD as determined by the immunohistochemistry with CD31 (CD31-MVD) and CD34 (CD34-MVD). VEGF showed a significant correlation with LAT1 expression ($P = 0.04$) and Ki-67 labeling index ($P = 0.01$); however it showed no correlation with patient age, gender, disease stage, tumor size, and histology. CD31-MVD and CD34-MVD showed no correlation with any parameters.

Correlation between angiogenesis and PET uptake. The maximal SUV of ^{18}F-FMT ranged from 0.81 to 3.60 (mean, 1.54 ± 0.53). The maximal SUV of ^{18}F-FDG ranged from 1.30 to 16.4 (mean, 6.97 ± 3.04). The maximal SUV of ^{18}F-FDG of primary tumor was significantly higher than that of ^{18}F-FMT ($P < 0.001$). Figure 3 shows the correlation of VEGF with ^{18}F-FMT and ^{18}F-FDG uptake. Maximal SUVs of ^{18}F-FMT and ^{18}F-FDG showed a significant correlation with VEGF ($\gamma = 0.5928$ [$P < 0.0001$] and $\gamma = 0.3657$ [$P = 0.026$], respectively), whereas they showed no correlation with CD31-MVD or CD34-MVD.

Correlation between angiogenesis and LAT1. LAT1 immunostaining revealed strong membranous staining carcinoma cells in tumor tissues (Fig. 1f). The cytoplasmic staining was rarely evident. A positive LAT1 expression was recognized in 70% (26/37) of 26 patients. The incidence of a positive LAT1 expression was significantly different between AC (8/17, 47%) and non-AC (18/20, 90%) ($P = 0.002$). The average score of the LAT1 expression was 2.9 ± 1.2 on a scale of 1 to 4. The LAT1 score was 2.5 ± 1.0 in AC and 3.5 ± 0.5 in non-AC. There was a significant difference in the LAT1 score between AC and non-AC ($P < 0.01$). A positive LAT1 expression was recognized in 60% (18/30) of patients with high VEGF expression and 14% (1/7) of low VEGF expression. There was a significant difference in the LAT1 expression between tumors with high VEGF and low VEGF expression ($P = 0.04$).

LAT1 showed a significant correlation with VEGF ($\gamma = 0.5509$, $P = 0.0004$), whereas it showed no correlation with CD31-MVD ($\gamma = 0.1713$, $P = 0.3106$) nor CD34-MVD ($\gamma = 0.1233$, $P = 0.4673$).

Correlation between angiogenesis and Ki-67 labeling index. The Ki-67 labeling index averaged 54 ± 22% (median, 54%) and ranged from 12% to 89% for the 37 patients. The Ki-67 labeling index was 38 ± 16% (median, 36%) in AC and 68 ± 22% (median,

doi: 10.1111/j.1349-7006.2008.01077.x

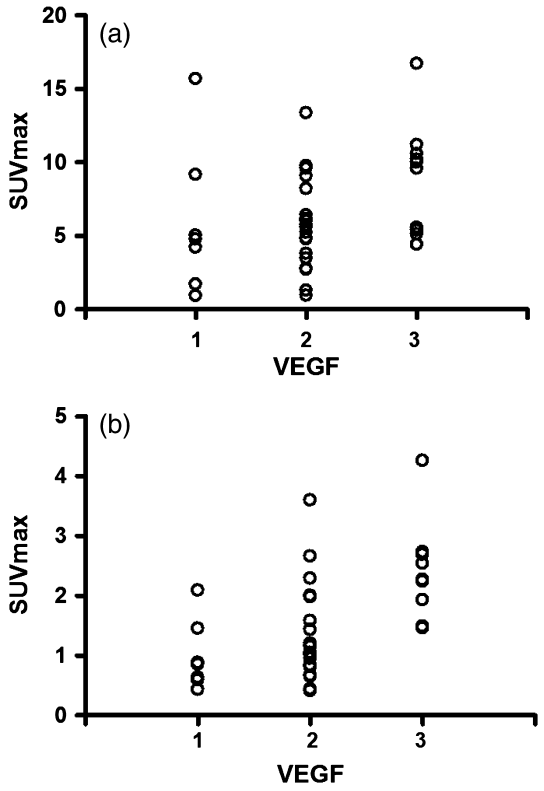

Fig. 3. Correlation between vascular endothelial growth factor (VEGF) expression and the metabolic activity of the tumor. Significant correlation is observed between VEGF and the standardized uptake value (SUVmax) of 2-[^{18}F]-fluoro-2-deoxy-D-glucose (^{18}F-FDG) ($\gamma = 0.3657$, $P = 0.026$) (a), VEGF and the uptake (SUVmax) of L-[3-^{18}F]-α-methyltyrosine (^{18}F-FMT) ($\gamma = 0.5928$, $P < 0.0001$) (b).

71%) in non-AC. The Ki-67 labeling index was significantly different between AC and non-AC ($P < 0.001$). High expression of Ki-67 was recognized in 90% (27/30) of tumors with high VEGF expression and 43% (3/7) of tumors with low VEGF expression. There was a significant difference in the LAT1 expression between tumors with high VEGF and low VEGF expression ($P = 0.01$). Ki-67 showed a significantly positive correlation with VEGF ($\gamma = 0.4565$, $P = 0.0045$), whereas it showed no correlation with CD31-MVD ($\gamma = 0.1942$, $P = 0.2495$) nor CD34-MVD ($\gamma = 0.1530$, $P = 0.3658$).

Correlation of PET uptake with Ki-67 labeling index and LAT1. Maximal SUVs of ^{18}F-FMT and ^{18}F-FDG showed a significant correlation with Ki-67 labeling index ($\gamma = 0.6755$ [$P < 0.0001$] and $\gamma = 0.6079$ [$P < 0.0001$], respectively) and LAT1 expression ($\gamma = 0.7658$ [$P < 0.0001$] and $\gamma = 0.5527$ [$P = 0.0004$], respectively), respectively.

Discussion

The present study demonstrated that the expression of VEGF was significantly correlated with ^{18}F-FMT and ^{18}F-FDG uptake. The VEGF expression seemed to be more closely correlated with ^{18}F-FMT uptake than ^{18}F-FDG uptake. The expression of VEGF had significant correlation with LAT1 which is specific to neoplastic cells and is a transporter of L-type amino acids such as L-tyrosine.

Angiogenesis is essential for neoplastic proliferation, progression, invasion, and metastasis because solid tumors cannot grow beyond 1–2 mm in diameter without angiogenesis.[21] Regarding the correlation between ^{18}F-FDG uptake and MVD in NSCLC, Tateishi *et al*. showed a positive correlation between ^{18}F-FDG uptake and CD34-MVD,[29] whereas Guo *et al*. showed a negative correlation between ^{18}F-FDG uptake and MVD (CD31 and CD34).[9] In the present study, no correlation was observed between ^{18}F-FDG uptake and MVD as determined by CD31 and CD34. This finding may be due to the common regulation of VEGF and Glut-1 by hypoxia-inducible factors (HIFs), which does not always relate with the increased angiogenesis. In contrast, ^{18}F-FDG uptake showed a significant correlation with VEGF expression and Ki-67 labeling index in the present study. These results suggest that the metabolic activity of a primary tumor as determined by the ^{18}F-FDG uptake is related to tumor angiogenesis and the proliferative activity in NSCLC. Up to now, a significant correlation was reported between ^{18}F-FDG uptake and VEGF expression in patients with breast cancer or esophageal cancer.[30,31] An experimental study revealed that ^{18}F-FDG uptake was significantly correlated with the expression of Glut-1 and the Glut-1 expression was coregulated with VEGF in both *in vitro* (lung cancer cell cultures) and *in vivo* (xenografts).[32] To our knowledge, there has been no published literature describing correlation of VEGF with ^{18}F-FDG uptake in NSCLC.

In the present study, VEGF expression showed a significant relationship with ^{18}F-FMT uptake and LAT1 expression. Our result suggests that amino acid transport system is related to tumor angiogenesis in NSCLC. While it is currently unclear why LAT1 is coveted by transformed cell, Fuchs *et al*. hypothesize that LAT1 provides the essential amino acids that act as signals to enhance growth of cancer cells via mammalian target-of-rapamycin (mTOR)-stimulated translation.[15] Likewise, mTOR regulates amino acid transporter gene expression and trafficking to the plasma membrane in response to the growth signal.[15] Moreover, overexpression of LAT1 was associated with metastasis *in vivo*.[33] Rapamycin has been shown to inhibit growth of metastatic tumors by angiogenesis.[34] These findings indicate that LAT1 expression is associated with angiogenesis to enhance cellular proliferation and metastasis. However, the exact molecular mechanism regulating LAT1 overexpression and angiogenesis remains to be clarified.

Funaioli C *et al*. reported that ^{18}F-FDG PET correlates better than computed tomography (CT) with pathological response to bevacizumab-based therapy in a patient with metastatic colon cancer.[35] In the present study, the correlation of VEGF and FDG was rather low and just reached statistical significance, whereas the correlation of FMT and VEGF seems to be more relevant. Since VEGF expression seems to be closely correlated with ^{18}F-FMT uptake, the clinical implication of the present results is that ^{18}F-FMT PET may be useful for monitoring the response to anti-angiogenic therapy in NSCLC. The clinical significance of ^{18}F-FMT PET is that the monitoring of anti-angiogenic therapy should be warranted in future studies.

One of the limitations of our study is that our sample size is small. The present study is preliminary, and further investigation with increased number of cases is mandatory. Next, we used maximal SUV as an uptake of PET tracers for comparison, but we could not confirm that the site of maximal SUV exactly corresponded to the site of highest angiogenesis in immunostaining. Another limitation is that we did not investigate the possible link between angiogenesis and prognosis. A further limitation is that our study did not evaluate the vascular endothelial growth factor (VEGF and VEGFR) family of proteins and receptors. This family comprises six secreted glycoproteins of which VEGF-A, VEGF-C and VEGF-D are of great significance.[36,37] These VEGF ligands mediate their angiogenic effect via the receptor tyrosine kinases VEGFR-1(flt-1), VEGFR-2 (KDR or Flk-1), and VEGFR-3 (Flt-4).[37] The relationship between VEGF family with LAT1 expression and prognostic role should be elucidated.

In conclusion, the present study demonstrated a significant correlation of VEGF expression with ^{18}F-FMT and ^{18}F-FDG uptake. The correlation of the uptake of ^{18}F-FMT and VEGF was more relevant, and LAT1 demonstrated a significant correlation with VEGF expression. The expression of VEGF was also correlated with cellular proliferation. These results suggest that ^{18}F-FMT PET may be useful for monitoring anti-VEGF therapy and for assessing metastatic potential and prognosis in patients with NSCLC.

Acknowledgments

We thank T. Hikino for technical assistance in the immunohistochemical staining of VEGF, CD31, CD34, LAT1 and Ki-67.

Conflicts of interest statement

We, all authors, have no financial or personal relationships with other people or organizations that could inappropriately influence our work.

References

1 Fontanini G, Lucchi M, Vignati S *et al*. Angiogenesis is a prognostic indicator of survival in non-small cell lung carcinoma: a prospective study. *J Natl Cancer Inst* 1997; **89**: 881–6.
2 Pastorino U, Andreola S, Tagliabue E *et al*. Immunocytochemical markers in stage I lung cancer: relevance to prognosis. *J Clin Oncol* 1997; **15**: 2858–65.
3 Yano T, Tanikawa S, Fujie T, Masutani M, Horie T. Vascular endothelial growth factor expression and neovascularisation in non-small cell lung cancer. *Eur J Cancer* 2000; **36**: 601–9.
4 Pieterman RM, van Putten JW, Meuzelaar JJ *et al*. Preoperative staging of non-small-cell lung cancer with positron-emission tomography. *N Engl J Med* 2000; **343**: 254–61.
5 Vansteenkiste JF, Stroobants SG, De Leyn PR *et al*. Lymph node staging in non-small-cell lung cancer with FDG-PET scan: a prospective study on 690 lymph node stations from 68 patients. *J Clin Oncol* 1998; **16**: 2142–9.
6 Brock CS, Meikle SR, Price P. Dose fluorine-18 fluorodexyglucose metabolic imaging of tumor benefit oncology? *Eur J Nucl Med* 1997; **24**: 691–705.
7 Higashi K, Ueda Y, Sakurai A *et al*. Correlation of Glut-1 glucose transporter expression with [^{18}F] FDG uptake in non-small cell lung cancer. *Eur J Nucl Med* 2000; **27**: 1778–85.
8 Higashi K, Ueda Y, Arisaka Y *et al*. ^{18}F-FDG uptake as a biologic prognostic factor for recurrence in patients with surgically resected non-small cell lung cancer. *J Nucl Med* 2002; **43**: 39–45.
9 Guo J, Higashi K, Ueda Y *et al*. Microvessel density: correlation with ^{18}F-FDG uptake and prognosis impact in lung adenocarcinomas. *J Nucl Med* 2006; **47**: 419–25.
10 Uchino H, Kanai Y, Kim DK *et al*. Transport of amino acid-related compounds mediated by l-type amino acid transporter 1 (LAT1): Insights into the mechanisms of substrate recognition. *Mol Pharmacol* 2002; **61**: 729–37.
11 Kim DK, Kanai Y, Choi HW *et al*. Characterization of the system L amino acid transporter in T24 human bladder carcinoma cells. *Biochim Biophys Acta* 2002; **1565**: 112–22.
12 Inoue T, Koyama K, Oriuchi N *et al*. Detection of malignant tumors: whole-body PET with fluorine-18-α–methyl tyrosine versus FDG-preliminary study. *Radiology* 2001; **220**: 54–62.
13 Kaira K, Oriuchi N, Otani Y *et al*. Diagnostic usefulness of fluorine-18-α-methyltyrosine positron emission tomography in combination with ^{18}F-fluorodeoxyglucose in sarcoidosis patients. *Chest* 2007; **131**: 1019–27.
14 Kaira k Oriuchi N, Otani Y *et al*. Fluorine-18-α-Methyltyrosine Positron Emission Tomography for Diagnosis and Staging of Lung Cancer: a clinicopathological study. *Clin Cancer Res* 2007; **13**: 6369–78.
15 Fuchs BC, Bode BP. Amino acid transporters ASCT2 and LAT1 in cancer: partners in crime? *Semin Cancer Biol* 2006; **15**: 254–66.
16 Giaccone G. The potential of antiangiogenic therapy in non-small cell lung cancer. *Clin Cancer Res* 2007; **13**: 1961–70.
17 Tomiyoshi K, Amed K, Muhammad S *et al*. Synthesis of new fluorine-18 labeled amino acid radiopharmaceutical: L-F-alpha-methyl tyrosine using separation and purification system. *Nucl Med Commun* 1997; **18**: 169–75.
18 Oriuchi N, Tomiyoshi K, Inoue T *et al*. Independent thallium-201 accumulation and fluorine-18-fluorodeoxyglucose metabolism in glioma. *J Nucl Med* 1996; **37**: 457–62.
19 Inoue T, Oriuchi N, Kunio M *et al*. Accuracy of standardized uptake value (SUV) measured by simultaneous emission and transmission scanning in PET oncology. *Nucl Med Commun* 1999; **20**: 849–57.
20 Mineo TC, Ambrogi V, Baldi A *et al*. Prognostic impact of VEGF, CD31, CD34, and CD105 expression and tumor vessel invasion after radical surgery for IB-IIA non-small cell lung cancer. *J Clin Pathol* 2004; **57**: 591–7.
21 Weidner N, Semple JP, Welch WR, Folkman J. Tumor angiogenesis and metastasis-correlation in invasive breast carcinoma. *N Engl J Med* 1991; **324**: 1–8.
22 Oda Y, Yamamoto H, Tamiya S *et al*. CXCR4 and VEGF expression in the primary site and the metastatic site of human osteosarcoma: analysis within a group of patients, all of whom developed lung metastasis. *Modern Pathol* 2006; **19**: 738–45.
23 Buck AC, Schirrmeister HH, Guhlmann CA *et al*. Ki-67 immunostaining in pancreatic cancer and chronic active pancreatitis: does in vivo FDG uptake correlate with proliferative activity? *J Nucl Med* 2001; **42**: 721–5.
24 Martin B, Paesmans M, Mascaux C *et al*. Ki-67 expression and patients survival in lung cancer: systematic review of the literature with meta-analysis. *Br J Cancer* 2004; **91**: 2018–25.
25 Yanagida O, Kanai Y, Chairoungdua A *et al*. Human 1-type amino acid transporter 1 (LAT 1): characterization of function and expression in tumor cell lines. *Biochim Biophys Acta* 2001; **1514**: 291–302.
26 Chairoungdua A, Segawa H, Kim JY *et al*. Identification of an amino acid transporter associated with the cystinuria-related type II membrane glycoprotein. *J Biol Chem* 1999; **274**: 28845–8.
27 Nawashiro H, Otani N, Shinomiya N *et al*. l-type amino acid transporter 1 as a potential molecular target in human astrocytic tumors. *Int J Cancer* 2006; **119**: 484–92.
28 Matsuo H, Tsukada S, Nakata T *et al*. Expression of a system L neutral amino acid transporter at the blood-brain barrier. *Neuroreport* 2000; **11**: 3507–11.
29 Tateishi U, Nishihara H, Tsukamoto E, Morikawa T, Tamaki N, Miyasaka K. Lung tumors evaluated with FDG-PET and dynamic CT. The relationship between vascular density and glucose metabolism. *J Comput Assist Tomogr* 2002; **26**: 185–90.
30 Bos R, van Der Hoeven JJ, van Der Wall E *et al*. Biologic correlates of ^{18}Fluorodeoxyglucose uptake in human breast cancer measured by positiron emission tomography. *J Clin Oncol* 2002; **20**: 379–87.
31 Choi JY, Jang KT, Shim YM *et al*. Prognostic significance of vascular endothelial growth factor expression and microvessel density in esophageal squamous cell carcinoma: comparison with positron emission tomography. *Ann Surg Oncol* 2006; **13**: 1054–62.
32 Pedersen MW, Holm S, Lund EL, Hojgaard L, Kristjansen PE. Coregulation of glucose uptake and vascular endothelial growth factor (VEGF) in two small-cell lung cancer (SCLC) sublines in vivo and in vitro. *Neoplasia* 2001; **3**: 80–7.
33 Tamai S, Masuda H, Ishii Y, Suzuki S, Kanai Y, Endou H. Expression of 1-type amino acid transporter 1 in a rat model of liver metastasis: positive correlation with tumor size. *Cancer Detect Prev* 2001; **25**: 439–45.
34 Guba M, von Breitenbuch P, Steinbauer M *et al*. Rapamycin inhibits primary and metastatic tumor growth by angiogenesis: involvement of vascular endothelial growth factor. *Nat Med* 2002; **8**: 128–35.
35 Funaioli C, Pinto C, Di Fabio F *et al*. ^{18}F-FDG PET evaluation correlates better than CT with pathological response in a metastatic colon cancer patient treated with bevacizumab-based therapy. *Tumori* 2007; **93**: 611–5.
36 Hicklin DJ, Ellis LM. Role of the vascular endothelial growth factor pathway in tumor growth and angiogenesis. *J Clin Oncol* 2005; **23**: 1011–27.
37 Donnem T, Al-Saad S, Al-Shibli K *et al*. Inverse prognostic impact of angiogenic marker expression in tumor cells versus stromal cells in non-small cell lung cancer. *Clin Cancer Res* 2007; **13**: 6649–57.

doi: 10.1111/j.1349-7006.2008.01077.x